Symmetry Reduction by Surface Scattering and Mobility Model for Stressed ⟨100⟩/(001) MOSFETs

F. M. Bufler*†, A. Erlebach†, and M. Oulmane†
*Institut für Integrierte Systeme, ETH Zürich, Gloriastrasse 35, CH-8092 Zürich, Switzerland
Email: bufler@iis.ee.ethz.ch
†Synopsys Schweiz GmbH, Thurgauerstrasse 40, CH-8050 Zürich, Switzerland
Email: {bufler, erlebach, oulmane}@synopsys.com

***Abstract*—It is demonstrated that the gate interface breaks the equivalence between vertical and transverse direction for the mobility in ⟨100⟩/(001) pMOSFETs, leading to 6 instead of 3 independent 1st order piezoconductance coefficients. This is found from Monte Carlo (MC) simulations yielding different effective mobilities for uniaxial vertical and transverse stress, which can be explained in terms of energy and parallel–momentum conservation upon specular surface scattering. A mobility model with stress–dependent 1st order piezoconductance coefficients is presented. This model is shown to reproduce well corresponding MC effective mobilities not only for low, but also for high stress.**

I. Introduction

Modeling the effective mobility as a function of stress for drift–diffusion (DD) device simulation is still a challenge because of the dependence of the mobiltiy on at least the three diagonal components of the stress tensor in device coordinates, in particular for holes with the complicated hole band structure. Existing interpolation–based models are mostly restricted to low stress with the piezoresistance coefficients obtained from measurements in bulk silicon [1], [2], from measurements in bulk MOSFETs (e.g. [3], [4]) or from simulating the inversion layer of bulk MOSFETs (e.g. [5], [6]). Physics–based models, on the other hand, have often been developed only for special stress configurations such as uniaxial longitudinal stress [7], [8] or biaxial stress [8]. In contrast, high stress levels are introduced in the channel of current short–channel devices by e.g. stressed nitride cap liners with the vertical stress component typically being dominant. This regime is not covered by any of the aforementioned models. It is therefore the aim of this paper to introduce an interpolation–based mobility model with stress–dependent piezoconductance coefficients for ⟨100⟩/(001) bulk MOSFETs in analogy to the corresponding model for ⟨110⟩/(001) bulk MOSFETs [9] the ⟨100⟩ channel orientation being used for low–power applications [10]. Furthermore, we explicitly show that surface scattering reduces the symmetry compared to bulk silicon. This increases the number of independent piezoconductance coefficients to be considered.

II. Monte Carlo Approach

Our model for the stress–induced mobility variation provides an interpolation between mobility enhancement data obtained from MC simulation. This section therefore summarizes the MC approach used to generate these effective mobility data. Self–consistent semiclassical MC simulations of an 0.5 μm bulk pMOSFET are being employed [11], i.e., the holes are simulated in a three–dimensional (3D) wave–vector ($\mathbf{k}$) space and in a two–dimensional (2D) real–space ($\mathbf{r}$). A six–band $\mathbf{k}\cdot\mathbf{p}$ band structure for strained silicon is used with values for valence–band parameters and deformation potentials as reported in Table I of Ref. [9]. The scattering mechanisms comprise optical and inelastic acoustic intra– and interband phonon scattering [12], screened ionized impurity scattering and surface roughness scattering. Surface roughness scattering consists of a combination of 85 % specular scattering, which is governed by the conservation of energy and parallel wave–vector of the hole upon hitting the gate oxide interface, and 15 % diffusive scattering. Quantum confinement is not taken into account. Therefore the perpendicular wave–vector component is well-defined and its value after specular surface scattering is found in the band structure table via the conservation of the energy and the parallel wave–vector. Because of the warped hole band structure, this mechanism does not imply the conservation of the parallel group velocity component as for a free particle with its parabolic band energy (see also the next section). It turned out that the resulting stress–induced effective hole mobility variations are relatively close to those reported for quantum–mechanical mobility calculations [5], [13] and corresponding wafer bending experiments [14] in ⟨110⟩/(001) MOSFETs under uniaxial stress [9]. Similar data are not available for the ⟨100⟩ channel orientation, but the bulk Monte Carlo simulations are in good agreement with the piezoresistance measurements [1] both for transport in crystallographic ⟨110⟩ and ⟨100⟩ direction [9].

The Monte Carlo simulations of the 0.5 μm bulk pMOSFET are performed at a low drain voltage of V_{DS}=0.1 V and the gate voltage V_{GS} is chosen such that it corresponds to the desired effective field strength. The effective field and

978-1-4244-7700-5/10/$26.00 ©2010 IEEE

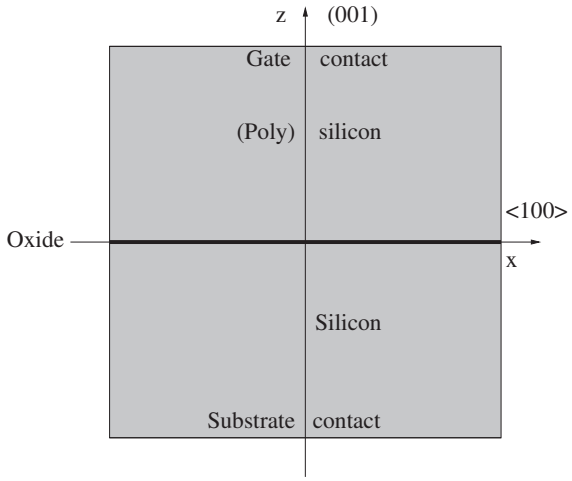

Fig. 1. Schematic of a ⟨100⟩/(001) MOSFET structure.

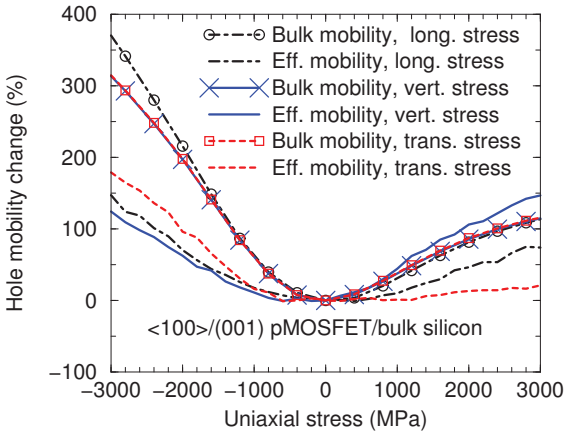

Fig. 2. Hole mobility change in bulk silicon and in a ⟨100⟩/(001) pMOSFET at an effective field of $E_{\rm eff}$ = 1.1 MV/cm for uniaxial stress in ⟨100⟩ transport or the two perpendicular directions according to bulk and device Monte Carlo simulation (longitudinal stress in ⟨100⟩ channel direction (dot-dashed line type, x–axis), vertical stress perpendicular to the gate interface in (001) substrate direction (solid line type, z–axis) and transverse stress (dashed line type, y–axis)). The bulk Monte Carlo simulation is performed at an electric field of 2 kV/cm.

the effective mobility are computed from internal quantities according to

$$E_{\rm eff} = \frac{q}{\epsilon_{\rm Si}} \int dz \big(N_{\rm D}^+ - n(x,z) - N_{\rm A}^- + \eta\, p(x,z) \big) \quad (1)$$

$$\mu_{\rm eff} = \frac{\int dz\, \frac{v_x(x,z)}{E_x(x,z)} p(x,z)}{\int dz\, p(x,z)}. \quad (2)$$

$N_{\rm D}^+$, n, $N_{\rm A}^-$ and p denote the donor, electron, acceptor and hole density, respectively, and η = 1/3 for the computation of the effective hole mobility. v_x and E_x are the x–components of the average hole velocity and of the electric field. The x–axis points in channel direction and integration over z is from the gate–oxide/silicon interface into the substrate. In the present study, the channel doping is given by $N_{\rm D}^+ = 2 \times 10^{17}$ cm^{-3} and $N_{\rm A}^-$ = 0.

III. Symmetry Reduction

Fig. 1 shows the schematic of a ⟨100⟩/(001) MOSFET. Here, the x, y and z coordinate axes are aligned with the crystallographic ⟨100⟩, ⟨010⟩ and ⟨001⟩ directions. Therefore the device and the crystallographic coordinate systems coincide and do not need to be distinguished in the following, in contrast e.g. to the case of a ⟨110⟩/(001) MOSFET [9]. The symmetry of bulk silicon is characterized by the 48 point operations of the cubic crystal. They can be classified by the elements corresponding to the 2^3=8 sign changes of the three coordinates ($\pm$ x, $\pm$ y, $\pm$ z) and to the 3!=6 coordinate permutations (x $\leftrightarrow$ y, x $\leftrightarrow$ z, y $\leftrightarrow$ z) and be represented by the corresponding 48 3×3 symmetry matrices. As a consequence of this symmetry, the mobility of unstrained bulk Si is isotropic and the piezoconductance tensor Π_{klij}, defined via the expansion of the relative mobility change tensor $\Delta\mu_{kl} \equiv (\mu_{kl} - \mu_{0,kl})/\mu_{0,kl}$

$$\Delta\mu_{kl} = \sum_{ij} \Pi_{klij} \sigma_{ij} \quad (3)$$

in terms of the stress tensor σ_{ij} up to the first order, contains only three independent coefficients. However, for particles propagating in the MOSFET structure shown in Fig. 1 this symmetry is reduced because the particles' wave–vector is changed by surface scattering when hitting the oxide at the xy–plane. As a consequence, the two coordinate permutations x $\leftrightarrow$ z and y $\leftrightarrow$ z are no longer a symmetry operation and therefore this structure has a reduced number of $2^3 \times 2!$ = 16 symmetry operations. From the viewpoint of symmetry this is the same situation as for a biaxially strained SiGe bulk alloy. This leads us to the conclusion that the same reduced symmetry has to be adopted for the piezoconductance tensor describing the stress–induced change of the effective mobility of an (001) MOSFET. Therefore the number of independent piezoconductance coefficients increases to six and Eq. (3) can be written in this case as

$$\begin{pmatrix} \Delta\mu_{xx} \\ \Delta\mu_{yy} \\ \Delta\mu_{zz} \\ \Delta\mu_{yz} \\ \Delta\mu_{xz} \\ \Delta\mu_{xy} \end{pmatrix} = \begin{pmatrix} \Pi_{11} & \Pi_{12} & \Pi_{13} & 0 & 0 & 0 \\ \Pi_{12} & \Pi_{11} & \Pi_{13} & 0 & 0 & 0 \\ \Pi_{13} & \Pi_{13} & \Pi_{33} & 0 & 0 & 0 \\ 0 & 0 & 0 & \Pi_{44} & 0 & 0 \\ 0 & 0 & 0 & 0 & \Pi_{44} & 0 \\ 0 & 0 & 0 & 0 & 0 & \Pi_{66} \end{pmatrix} \begin{pmatrix} \sigma_{xx} \\ \sigma_{yy} \\ \sigma_{zz} \\ \sigma_{yz} \\ \sigma_{xz} \\ \sigma_{xy} \end{pmatrix}$$

using the conventional tensor contraction [15].

These symmetry considerations are supported by the comparison of the MC computed effective and bulk hole mobility enhancements shown in Fig. 2 for uniaxial longitudinal, vertical, and transverse stress. The analogous comparison of the MC effective mobility with the results of the bulk piezoresistance model [1] is displayed in Fig. 3. It can be seen that the mobility changes of both the bulk MC model and the bulk piezoresistance model are the same for vertical and transverse stress, because the crystallographic ⟨001⟩ and ⟨010⟩ directions are equivalent. In contrast, the effective MC mobilities are different for vertical and transverse stress, especially for tensile stress. This implies in particular $\Pi_{13} \neq \Pi_{12}$. The reason for

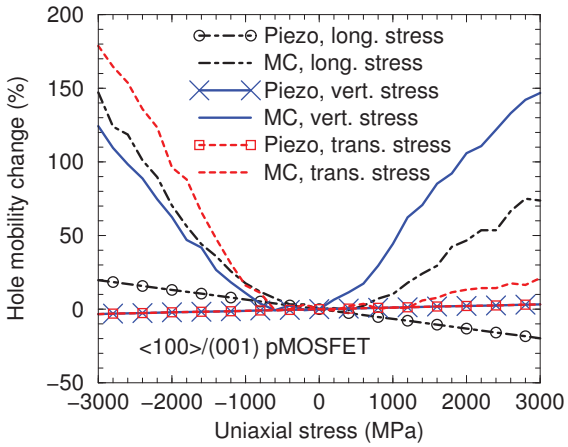

Fig. 3. Effective hole mobility change in a ⟨100⟩/(001) pMOSFET at an effective field of $E_{\rm eff}$ = 1.1 MV/cm according to bulk piezoresistance [1] and Monte Carlo device simulation for three uniaxial stress directions.

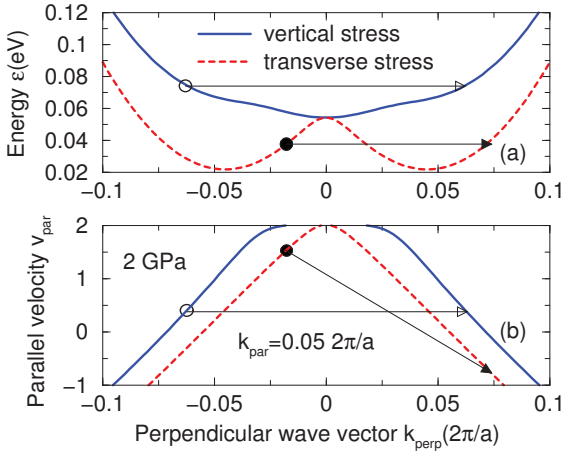

Fig. 4. Heavy–hole energy ϵ (a) and group velocity component parallel to the surface $v_{\rm par}$ (b) both as a function of the wave vector component perpendicular to the surface $k_{\rm perp}$ with the wave vector component parallel to the surface fixed at $k_{\rm par}$= 0.05 × 2π/a for transverse and vertical stress direction.

this effect is that energy and parallel–momentum conservation upon specular surface scattering allow for transverse stress the reversal of the parallel velocity component thus reducing the effective mobility compared to vertical stress. This mechanism is exemplified in Fig. 4 illustrating the transition of a hole between its state before and after specular scattering. Conservation of parallel crystal momentum and energy requires that the parallel crystal momentum component remains fixed and that possible values for the after–scattering perpendicular crystal momentum component are intersection points between the equienergy lines and the energy dispersion curves in Fig. 4 (a). From Fig. 4 (b) one can obtain the corresponding values of the associated parallel group velocity component. While the value of the parallel velocity does not change for the case of vertical stress, it can even change the sign and become negative for transverse stress. Such strong effects of this mechanism had been previously found for SiGe pMOSFETs [16] and for unstrained–Si pMOSFETs with different crystallographic surface orientations [17]. In particular, the order and the dependence of the effective hole mobility change on surface and channel orientation was in good agreement with corresponding measurements [17] validating this concept also from an experimental point of view. Note that the different effective hole mobilities for uniaxial transverse and vertical stress result from the same band structure table. As for the case of the orientation dependence of the unstrained–Si mobility [17], the different effect comes about only by a different orientation of the same band structure with respect to the gate interface.

From a mathematical viewpoint, the surface scattering mechanism described above corresponds to a boundary condition for the Boltzmann equation at an insulator interface [18]. Hence, the symmetry reduction of transport in a MOS system is due to a boundary condition of the Boltzmann equation in conjunction with a warped band structure, occurring within semiclassical transport without consideration of quantization.

IV. Mobility Model for ⟨100⟩/(001) MOSFETs

The quantity of interest is only the mobility change in channel direction and we are therefore left with the equation

$$\Delta\mu_{xx} = \Pi_{11}\sigma_{xx} + \Pi_{12}\sigma_{yy} + \Pi_{13}\sigma_{zz}. \qquad (4)$$

While Eq. (4) contains the correct symmetry, it is only valid for low stress. Our ansatz to extend the validity to higher stress consists of introducing a stress–dependence of the piezoconductance coefficients according to

$$\Pi_{11} = \Delta'_{(\sigma 00)}(\sigma_{xx}) \equiv \Delta\mu_{xx}(\sigma_{xx},0,0)/\sigma_{xx} \qquad (5)$$
$$\Pi_{12} = \Delta'_{(0\sigma 0)}(\sigma_{yy}) \equiv \Delta\mu_{xx}(0,\sigma_{yy},0)/\sigma_{yy} \qquad (6)$$
$$\Pi_{13} = \Delta'_{(00\sigma)}(\sigma_{zz}) \equiv \Delta\mu_{xx}(0,0,\sigma_{zz})/\sigma_{zz}, \qquad (7)$$

where the three effective mobility change curves are taken from the corresponding Monte Carlo results shown in Figs. 2 and 3 for the three uniaxial stress conditions.

By construction, the results of the mobility model defined via the Eqs. (4), (5), (6) and (7) coincide with the MC results for the three uniaxial stress configurations and yield accurate mobilities for arbitrary, but low stress due to the correct symmetry. For general situations with high stress levels, the model provides an interpolation between the MC mobility curves for uniaxial longitudinal, vertical and transverse stress. In order to test its accuracy, we compare in Figs. 5 and 6 the new model with effective long–channel MC mobilities for typical stress tensors as obtained from mechanical stress simulation for dual stress liner (DSL) [19] or etch stop liner (ESL) [20] situations. In contrast to the linear piezoresistance model [1], both trends and magnitude of the MC results are overall well captured, thus validating the proposed approach. Hence, stress–dependent 1st order coefficients are sufficient in contrast to the case of ⟨110⟩/(001) pMOSFETs [9] where also 2nd order terms were necessary for sufficient accuracy. The present model for the effective low–field mobility refers to inversion conditions ($E_{\rm eff}$ = 1.1 MV/cm), but extensions are

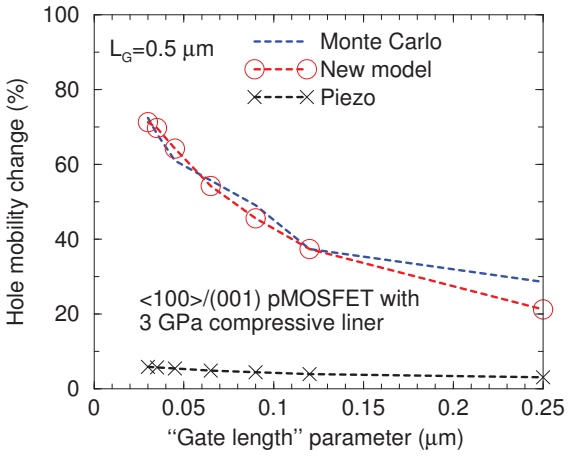

Fig. 5. Effective long–channel hole mobility change according to Monte Carlo simulation, the new hole mobility model and the linear piezoresistance model [1] for different stress configurations. The stress components correspond to gate length dependent mechanical stress simulation using as stressor a 60 nm thick compressive nitride cap liner with an intrinsic stress of - 3 GPa [19]. The "gate length" only serves to parametrize the stress tensor.

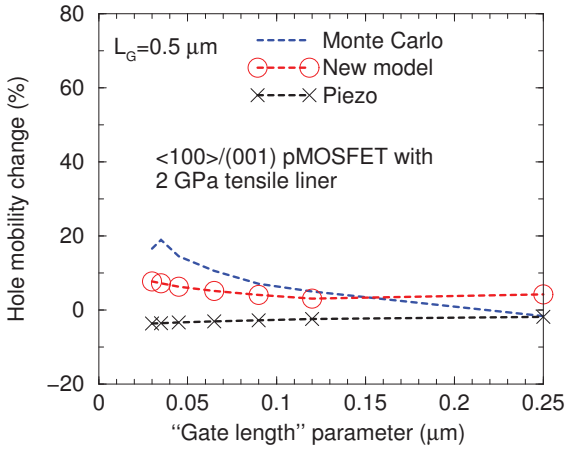

Fig. 6. Effective long–channel hole mobility changes as in Fig. 5, but using as stressor a 60 nm thick tensile nitride cap liner with an intrinsic stress of 2 GPa [20].

possible to include further dependencies on e.g. the effective field or the germanium content in SiGe pMOSFETs. It can be used in DD simulation together with the Caughey–Thomas expression for high–field saturation where the total mobility enhancement is smaller due to the stress–independence of the saturation velocity.

V. Conclusion

It was shown that surface scattering reduces the symmetry for transport in MOSFET structures compared to bulk silicon as a result of the boundary condition for the Boltzmann equation at insulating contacts in conjunction with warped band structures. The reduced symmetry was used to formulate an effective low–field mobility model with stress–dependent 1st order piezoconductance coefficients which can be used for DD simulation of ⟨100⟩/(001) pMOSFETs.

References

[1] C. S. Smith, "Piezoresistance effect in germanium and silicon," *Phys. Rev.*, vol. 94, pp. 42–49, 1954.

[2] K. Matsuda, K. Suzuki, K. Yamamura, and Y. Kanda, "Nonlinear piezoresistance effects in silicon," *J. Appl. Phys.*, vol. 73, pp. 1838–1847, 1993.

[3] S. E. Thompson, G. Sun, Y. S. Choi, and T. Nishida, "Uniaxial-process-induced strained-Si: Extending the CMOS roadmap," *IEEE Trans. Electron Devices*, vol. 53, pp. 1010–1020, 2006.

[4] K. Huet, M. Feraille, D. Rideau, R. Delamare, V. Aubry-Fortuna, M. Kasbari, S. Blayac, C. Rivero, A. Bournel, C. Tavernier, P. Dollfus, and H. Jaouen, "Experimental and theoretical analysis of hole transport in uniaxially strained pMOSFETs," in *Proc. ESSDERC*, Edinburgh (UK), Sep. 2008, pp. 234–237.

[5] G. Sun, Y. Sun, T. Nishida, and S. E. Thompson, "Hole mobility in silicon inversion layers: Stress and surface orientation," *J. Appl. Phys.*, vol. 102, 084501, 2007.

[6] A. T. Pham, C. Jungemann, and B. Meinerzhagen, "Modeling of piezoresistive coefficients in Si hole inversion layers," in *Proc. ULIS*, Aachen (Germany), Mar. 2009, pp. 121–124.

[7] B. Obradovic, P. Matagne, L. Shifren, X. Wang, M. Stettler, J. He, and M. D. Giles, "A physically-based analytic model for stress-induced hole mobility enhancement," *J. Comput. Electron.*, vol. 3, pp. 161–164, 2004.

[8] S. Reggiani, L. Silvestri, A. Cacciatori, E. Gnani, A. Gnudi, and G. Baccarani, "Physically–based unified compact model for low–field carrier mobility in MOSFETs with different gate stacks and biaxial/uniaxial stress conditions," in *IEDM Tech. Dig.*, 2007, pp. 557–560.

[9] F. M. Bufler, A. Erlebach, and M. Oulmane, "Hole mobility model with silicon inversion layer symmetry and stress-dependent piezoconductance coefficients," *IEEE Electron Device Lett.*, vol. 30, pp. 996–998, 2009.

[10] J. Yuan, V. Chan, N. Rovedo, V. Sardesai, N. Kanike, V. Varadarajan, M. Yu, J. H. Yang, Y. K. Jeong, O. S. Kwon, M. P. Belyansky, M. Eller, Y. M. Lee, N. Cave, H. Shang, Y. Li, and R. Divakaruni, "Blanket SMT with In Situ N2 plasma treatment on the ⟨100⟩ wafer for the low-cost low-power technology application," *IEEE Electron Device Lett.*, vol. 30, pp. 916–918, 2009.

[11] F. M. Bufler, A. Tsibizov, and A. Erlebach, "Scaling of bulk pMOSFETs: (110) surface orientation versus uniaxial compressive stress," *IEEE Electron Device Lett.*, vol. 27, pp. 992–994, 2006.

[12] F. M. Bufler, A. Schenk, and W. Fichtner, "Simplified model for inelastic acoustic phonon scattering of holes in Si and Ge," *J. Appl. Phys.*, vol. 90, pp. 2626–2628, 2001.

[13] P. Packan, S. Cea, H. Deshpande, T. Ghani, M. Giles, O. Golonzka, M. Hattendorf, R. Kotlyar, K. Kuhn, A. Murthy, P. Ranade, L. Shifren, C. Weber, and K. Zawadzki, "High performance Hi-K + metal gate strain enhanced transistors on (110) silicon," in *IEDM Tech. Dig.*, 2008, pp. 63–66.

[14] E. X. Wang, P. Matagne, L. Shifren, B. Obradovic, R. Kotlyar, S. Cea, M. Stettler, and M. D. Giles, "Physics of hole transport in strained silicon MOSFET inversion layers," *IEEE Trans. Electron Devices*, vol. 53, pp. 1840–1851, 2006.

[15] J. Richter, O. Hansen, A. N. Larsen, J. L. Hansen, G. F. Eriksen, and E. V. Thomsen, "Piezoresistance of silicon and strained $Si_{0.9}Ge_{0.1}$," *Sens. Actuators: Phys. A*, vol. 123–124, pp. 388–396, 2005.

[16] C. Jungemann, S. Keith, and B. Meinerzhagen, "Full–band Monte Carlo simulation of a 0.12 μm–Si–PMOSFET with and without a strained SiGe–channel," in *IEDM Tech. Dig.*, 1998, pp. 897–900.

[17] F. M. Bufler and A. Erlebach, "Monte Carlo simulation of the performance dependence on surface and channel orientation in scaled pFinFETs," in *Proc. ESSDERC*, Montreux (Switzerland), Sep. 2006, pp. 174–177.

[18] D. Schroeder, *Modelling of Interface Carrier Transport for Device Simulation*. Wien: Springer, 1994.

[19] F. M. Bufler, R. Gautschi, and A. Erlebach, "Monte Carlo stress engineering of scaled (110) and (100) bulk pMOSFETs," *IEEE Electron Device Lett.*, vol. 29, pp. 369–371, 2008.

[20] F. M. Bufler, F. O. Heinz, A. Tsibizov, and M. Oulmane, "Simulation of ⟨110⟩ nMOSFETs with a tensile strained cap layer," *ECS Trans.*, vol. 16, no. 10, pp. 91–100, 2008.